Denoised Predictions: Combining Information Bottleneck and Predictive Information to learn denoised representations

Anonymous authors
Paper under double-blind review

Abstract

Humans excel at isolating relevant information from noisy data to predict the behavior of dynamic systems, effectively disregarding non-informative, temporally-correlated noise. In contrast, existing reinforcement learning algorithms face challenges in generating noise-free predictions within high-dimensional, noise-saturated environments, especially when trained on world models featuring realistic background noise extracted from natural video streams. We propose a novel information-theoretic approach that learn world models based on minimising the past information and retaining maximal information about the future, aiming at simultaneously learning control policies and at producing denoised predictions. Utilizing Soft Actor-Critic agents augmented with an information-theoretic auxiliary loss, we validate our method's effectiveness on complex variants of the standard DeepMind Control Suite tasks, where natural videos filled with intricate and task-irrelevant information serve as a background. Experimental results demonstrate that our model outperforms nine state-of-the-art approaches in various settings where natural videos serve as dynamic background noise. Our analysis also reveals that all these methods encounter challenges in more complex environments.

1 Introduction

A major open problem in Reinforcement learning (RL) is to learn the dynamics and control policies from the high-dimensional observations such as images (Ha & Schmidhuber, 2018; Lillicrap et al., 2016; Hafner et al., 2020a; 2021a; Hansen et al., 2022). Conventionally, it is assumed that the observations in the environment, often derived through hand-engineered features, consist exclusively of task-relevant information. This allows RL algorithms to operate in a controlled setting with optimal efficiency, primarily due to the absence of exogenous noise (unrelated or uncontrollable external variables such as weather variations or random background movements), that could potentially hinder the learning process.

In the real world, the landscape is vastly different, brimming with a plethora of information, much of

Figure 1: **Top Row:** Ground truth data from a random sequence. **Bottom Row:** Reconstruction from DP.

which is irrelevant to a specific task. The challenge lies in accurately identifying task-relevant information and avoid the modeling of temporally correlated dynamics of the background noise. Prior RL methodologies (Yarats et al., 2021; Hafner et al., 2020a; Ha & Schmidhuber, 2018) that derive representations directly from observations, often integrate task-irrelevant information into their representations. They struggle to disentangle the noise from relevant information, unnecessarily modeling noise dynamics, leading to sub-optimal performance under noise (see Figure 7).
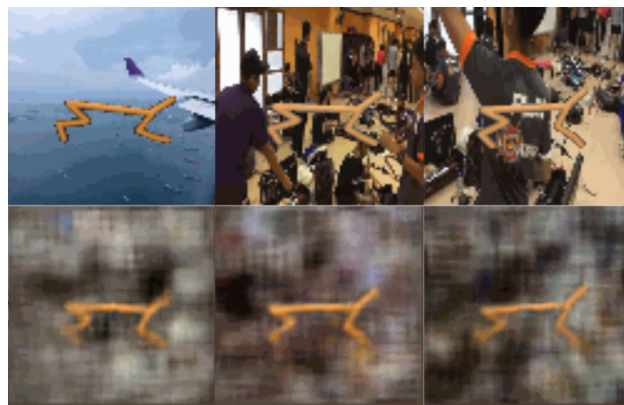
The process of computing representations relies on the past inputs, while the imagination and exploration are directed towards future (Hafner et al., 2020b). Our objective is to develop a cohesive perspective on how an agent formulates its current representation after observing past inputs and before observing future. Could it be feasible to model this process as an information flow, transitioning from past to future, mediated by the current state?

We introduce **De**noised **Pre**dictions (DePre), a model-based reinforcement learning approach that leverages information theory to learn robust and meaningful representations. DePre models Predictive Information (Bialek & Tishby, 1999), the mutual information between the past and the future, and employs the Information Bottleneck principle (Tishby et al., 2000) to derive a compact representation of the current state from historical observations, while preserving maximal predictive information about future outcomes. Essentially, DePre focuses on learning a concise abstraction of the system dynamics and leverages it to learn control policies and generate noise-free future predictions. This is achieved through deriving an objective integrating two central ideas: minimization of mutual information about past and the maximization of predictive ability for future. This dual objective consists of two contrastive losses and is formulated as a single optimization problem. While in this paper we focus on the algorithmic derivation and the performance of DePre, the information theoretic nature of it enables future investigations of generalization, stability and robustness aspects. The primary contributions of our work are as follows:

1. Our work is the first to illustrate that denoised state representations can be derived effectively through the preservation of predictive information.

2. Implicitly integrating a variety of methodologies from previous works, the paper presents a theoretical generalized framework for world model learning in the context of bottleneck methods.

3. DePre outperforms nine existing approaches on a majority of modified DeepMind control (DMC) tasks. We also show that along with learning dynamics, it can also produce better noise-free predictions than its counterparts.

2 Related Work

In this section, we delve into related work on reinforcement learning from visual input, focusing specifically on model-based approaches and representation learning concepts.

2.1 Model-based Reinforcement Learning.

These models simultaneously learn policy and transition dynamics, which can be used for planning, and are often sample efficient due to their ability to handle rich observations (Kaiser et al., 2020; Chua et al., 2018; Hafner et al., 2019; Ebert et al., 2018; Lowrey et al., 2019; Gelada et al., 2019; Lee et al., 2020a). World Models Ha & Schmidhuber (2018) uses recurrent latent model to imagine future frames. Stochastic Optimal control with Latent Representations (SOLAR) Zhang et al. (2019) model dynamics with linear-quadratic regulator. In particular, Dreamer Hafner et al. (2020a) optimises policies via backpropagating through latent dynamics and uses recurrent state-space model for planning in latent space. These reconstruction-based methods perform effectively in standard environments. However, when exposed to environments with noise distractors, they struggle to bifurcate between information they should reconstruct and what they should disregard.

2.2 Learning Representations and RL.

Recent works (Chen et al., 2020; Henaff, 2020; Tian et al., 2020) have demonstrated progress in learning representations from unlabeled data. These concepts have been integrated into reinforcement learning by works like (Laskin et al., 2020; Oord et al., 2018; Shu et al., 2020; Ma et al., 2021; Oord et al., 2018; Ma et al., 2021; Hjelm et al., 2019). Learning invariant representations with Information-theoretic constraints have been extensively used in the literature. However, the challenge of identifying and effectively utilizing task-relevant information, which necessitates not only the preservation of predictive information but also the generation

of noise-free predictions, remains largely unaddressed by most existing methods that predominantly rely on auxiliary decoders. Our concept shares similarities with PI-SAC (Lee et al., 2020b), whose objective is also centered around Predictive Information. PI-SAC aims to identify a latent representation of the current state that reduces the MI between past observations and actions $I(o_{t^-}; z_{t^-}|a_{t^-})$, while simultaneously maximising the MI between all future observations and rewards, represented as $I(o_{t^+}; r_{t^+})$. Notably, the authors of PI-SAC present this objective straightforwardly, without an underlying mathematical derivation of selection of the variables. In contrast, our method is underpinned by a solid theoretical foundation, where objectives related to latent representations and actions emerge implicitly. Furthermore, we incorporate a historical variable that circumvents the need to consider the entire trajectory by accumulating all the information in that variable, which solves the problem of considering the entire trajectory. Empirically, it has been shown in numerous previous papers that PI-SAC underperforms in scenarios involving distractors Wang et al. (2022); Liu et al. (2024), underscoring the robustness and effectiveness of our approach in such complex environments. Unlike strategies such as Dynamic Bottleneck (DB) Bai et al. (2021) and Sequential Information Bottleneck (SIBE) You et al. (2022), our approach not only seeks compact representations under noisy conditions, but also emphasizes on achieving noiseless future predictions and treating temporal noise along representations.

2.3 Learning Control from pixels with distractors.

Recent developments in model-based RL (Zhang et al., 2021; Ma et al., 2021; Nguyen et al., 2021; Fu et al., 2021; Bai et al., 2021; You et al., 2022; Bharadhwaj et al., 2022; Wang et al., 2022; Islam et al., 2022; Tomar et al., 2023; Liu et al., 2024) have put forward a variety of innovative ideas aimed at extracting relevant information from observations. Contrastive Variational Reinforcement Learning (CVRL) Ma et al. (2021) aims at maximises the MI between observations and representations i.e. $I(o_t, z_t)$, which is exactly similar to our objective "Predictive Observation Model" in Equation 3 (except we consider it for all the timesteps and not just a single instance) and leverages InfoNCE contrastive loss Oord et al. (2018) to optimise the objective. However, it does not address any objective related to generating noise-free dynamics or predictions, which can be observed via the reconstruction results in the original paper Ma et al. (2021) (Figure 3, Page 7). MIRO Ding et al. (2020) is another method that bears a close resemblance to CVRL. However, unlike CVRL, MIRO focuses on maximizing the mutual information (MI) between the state and observation, conditioned on the given action and constrained by dynamic predictions. Deep Bisimulation for Control (DBC) Zhang et al. (2021) learns control policies by learning representations of the states that preserve the bisimulation metric. Temporal Predictive Coding (TPC) Nguyen et al. (2021) shares conceptual similarities with our approach, striving to eliminate temporal noise while focusing only on the relevant aspects. The goal of TPC is to maximize the MI between future latent codes and the combination of prior latent codes and action tuples. This objective is achieved through contrastive learning, which exhibits a mathematical resemblance to Equation 10. More recent methods such as Task Informed Abstractions (TIA) Fu et al. (2021) maintain two separate latent models, one for tasks and another for distractors, bifurcating noise and signal. TIA falters in achieving better rewards when the grayscale background is replaced with RGB (see the experimental section). InfoPower Bharadhwaj et al. (2022) Iso-Dreamer Pan et al. (2022) learns inverse dynamics model to understand the controllable and non-controllable state-action relationship. It then aims to decouple these dynamics by rolling out their latent representations into the future to understand how these dynamics influence current behavior. Our work bypasses the need for explicitly defining these types of model rules and instead builds on a general information-theoretic model wherein these types of features implicitly emerge.

3 Notation and Preliminaries

3.1 Reinforcement Learning.

An agent operates in a Markov Decision Process (MDP), which is characterised by a tuple $\mathcal{M} = (\mathcal{O}, \mathcal{A}, \mathcal{P}, \mathcal{R}, \gamma)$, consisting of the observation space $\mathcal{O}$ with observations o (we interchangeably use "states" and "observations"), action space $\mathcal{A}$ with actions a, transition dynamics $\mathcal{P}$, Reward space $\mathcal{R}$ and discount factor $\gamma \in [0, 1]$. The encoder $\phi(z|o)$ produces a latent representation z from observations, and then the

policy $\pi(a|z)$ decodes this latent representation into actions. The goal of RL is to learn a policy $\pi^*(a|z)$ that maximizes the expected cumulative discounted rewards $\mathbb{E}_p\left[\sum_t \gamma^t r_t\right]$.

3.2 Predictive Information.

Predictive Information (PI) is a quantity that measures how much our observations from the past can inform us about the future Bialek & Tishby (1999) . Mathematically, it can be defined as the mutual information (MI) between the past (x_{past}) and the future (x_{future}), denoted as $I(x_{past}; x_{future})$. Assuming temporal invariance (any fixed time length is expected to have the same entropy), PI becomes a subextensive quantity, as expressed by $\lim_{T\to\infty} I(T)/T = 0$, where $I(T)$ is the predictive information over a time window of length 2T (with T steps of the past predicting T steps into the future), see Equation 3.1 in Bialek et al. (2001). As the time frame increases, the past contains a diminishing predictive value for the future. In order to capture only the necessary information from x_{past} for predicting x_{future}, a compressed representation of x_{past} is required.

3.3 Information Bottleneck.

For learning this compressed representation, we utilize the Information Bottleneck (IB) principle Tishby et al. (2000). IB aims at learning a representation z that aims to optimally compress the information provided by the input $x \in X$, i.e. minimize $I(x; z)$, while still maintaining enough knowledge to predict the outcome $y \in Y$, i.e. maximize $I(z; y)$. This objective is unified with the inclusion of a Lagrangian multiplier and formalized as $max\ I(z; y) - \beta I(x; z)$. The parameter β controls the information flow from the input x to the latent representation, balancing the trade-off between information preservation and compression.

4 Denoised Predictions

Denoised Predictions (DePre) is an information theory-based approach, that encapsulates the notions of predictive information and the information bottleneck. This core idea enables the learning of a compressed representation from high-dimensional observations, distilling task-relevant details from past observations, and leveraging this refined knowledge for future predictions while effectively filtering out noise. We hypothesise that the current state should encapsulate the requisite and meaningful information essential to perform the task. If the information is insufficient, the latent representations may fail to capture all the task-relevant information, leading to sub-optimal learning outcomes. On the other hand, if we incorporate an overabundance of information, our representations could become encumbered with noise-related artifacts that results in a dilution of task-relevant data and in a performance decrease.

We denote the latent representations for the past observations by o_{t-}, current observation by o_t, and the future observations by o_{t+}. We use z_{t-}, z_t and z_{t+} respectively for the latent space. For consistency and clarity, we establish that the episode initiates at time $t = 1$ and terminates at the horizon $t = T$. The objective is to encode observations (o_{t-}, o_t) into latent representations (z_{t-}, z_t), transform them to next state representations z_{t+}, and decode into future observations o_{t+} (Figure 2). Consequently, this process creates a two-fold bottleneck: one while transforming observations into latent representations and vice-versa $(o_t \leftrightarrow z_t)$, and another when acquiring the latent representation itself from other latent representations $(z_{t-1} \to z_t \to z_{t+1})$. In this context, our transition function can be conceptualized as a model operating simultaneously as an encoder and a decoder, encoding z_t from z_{t-} and decoding z_t to yield z_{t+}, with bottleneck being z_t.

Intuitively, we obtain task-relevant information from raw observations into our latent representations by minimising mutual information $I(o_{t-}, o_t; z_{t-}, z_t)$ while maximising the mutual information $I(o_t, o_{t+}; z_t, z_{t+})$, which preserves the predictive information for the reverse scenario. This can be written as,

$$\min\ I(o_{t-,t}; z_{t-,t}) - \beta_1 I(o_{t,t+}; z_{t,t+}). \tag{1}$$

In order to learn temporal abstractions and compressed representations from a sequence of past states and acquire relevant predictions, we employ the principle of Information Bottleneck, aiming to minimize $I(z_{t-}; z_t)$

and maximize $I(z_t; z_{t+})$,

$$\min \ I(z_{t-}; z_t) - \beta_2 I(z_t; z_{t+}). \tag{2}$$

Merging objectives from equation (1) and (2), we obtain a unified optimizing problem,

$$\min \ \Big[\ \underbrace{I(o_{t-,t}; z_{t-,t})}_{\substack{\text{Historical} \\ \text{observation model}}} + \ \underbrace{I(z_{t-}; z_t)}_{\substack{\text{Historical latent} \\ \text{space dynamics}}} \ \Big] - \Big[\underbrace{\beta_1 I(o_{t,t+}; z_{t,t+})}_{\substack{\text{Predictive} \\ \text{observation model}}} + \ \underbrace{\beta_2 I(z_t; z_{t+})}_{\substack{\text{Predictive latent} \\ \text{space dynamics}}} \ \Big], \tag{3}$$

where β_1 and β_2 can be seen as Lagrangian multipliers as mentioned in (Tishby et al., 2000). This implies that the problem can be optimised by minimizing the upper bound associated with the past, as represented by the first two terms, and simultaneously maximizing the lower bound related to the future, embodied in the final two terms. The objective of our DePre considers action dependencies implicitly through the latent space representations, $p(z_t|z_{t-}, a_{t-})$, thereby reflecting the innate characteristics of system transitions. This compatibility with RL principles facilitates a seamless integration of our approach into existing RL algorithms, where DePre can serve as an auxiliary function, significantly enhancing the learning of representations.

4.1 State Space Model

We use the state-space model described in Figure 2 with,

Encoder Representation: $z_t \sim p_\varphi(z_t \mid o_t)$
Transition dynamics: $z_{t+1} \sim q_\theta(z_{t+1} \mid z_t, a_t, h_t)$
Observation model: $o_t \sim r_\psi(o_t \mid z_t)$
History model: $h_t \sim p(h_t \mid h_{t-1}, a_{t-1})$. $\quad$ (4)

The conditional $p(h_t \mid h_{t-1}, a_{t-1})$ denotes the history model, that encapsulates the past variables into a single history variable i.e.,

$$h_t = \{z_{t-1}, a_{t-1}, ..., z_1, a_1\},$$
$$= \{z_{t-1}, a_{t-1}, h_{t-1}\}. \tag{5}$$

This is a crucial modelling component that is discussed and used in the next subsections.
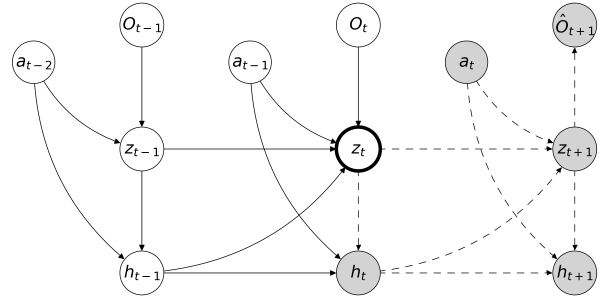

Figure 2: **State-space model.** The variable z_t acts as a bottleneck for the model, serving as a critical link between the historical (white circles) and predictive elements (grey circles). Solid edges designate the inputs required for inference, while the dotted edges represent the generative components.

4.2 Minimising the upper bound of the Past Mutual Information

This subsection discusses the minimization of the first two terms of DePre in Equation 3.

4.2.1 Upper bound of historical latent space dynamics.

We aim at minimising the tractable upper bound on the mutual information $I(z_{t-}; z_t)$. The mutual information can be represented as,

$$I(z_{1:t}) = \mathbb{E}_{p(z_{1:t})} \left[\log \frac{p(z_{1:t})}{\prod_{k=1}^{t} p(z_k)} \right],$$

We incorporate actions into the model by introducing a conditional probability distribution $p(z_{t-}, z_t | a_{t-})$,

$$I(z_{1:t}) = \mathbb{E}_{p(z_{1:t}, a_{1:t-1})} \left[\log \frac{p(z_{1:t}) p(z_{1:t}|a_{1:t-1})}{p(z_{1:t}|a_{1:t-1}) \prod_{k=1}^{t} p(z_k)} \right] \leq \mathbb{E}_{p(z_{1:t}, a_{1:t-1})} \left[\log \frac{p(z_{1:t}|a_{1:t-1})}{\prod_{k=1}^{t} p(z_k)} \right]. \tag{6}$$

Utilising the chain rule in conditional probability and for every t, substituting $\{z_{t-1}, a_{t-1}, h_{t-1}\}$ as h_t like Equation (5), we can write Equation (6) as

$$I(z_{1:t}) \leq \sum_{k=1}^{t-1} \mathbb{E}_{p(z_k, a_k)} \left[\log \frac{p(z_{k+1}|z_k, a_k, h_k)}{p(z_{k+1})} \right] = \sum_{k=1}^{t-1} I\big(z_{k+1}; z_k, a_k, h_k\big). \tag{7}$$

In essence, this implies that we can optimize the mutual information between the past latent representations and the present state's representation by minimising the upper bound of the MI for each individual, independent transition in a Markovian manner.

4.2.2 Upper bound of the historical observation model.

As in the previous section, it can be shown that an upper bound for $I(o_{1:t}, z_{1:t})$ can be derived by introducing the conditional distribution $p(z_{t^-}, z_t|a_{t^-})$,

$$I(o_{1:t}; z_{1:t}) \leq \mathbb{E}_{p(z_{1:t}, o_{1:t})} \left[\log \frac{p(z_{1:t}|o_{1:t})}{p(z_{1:t}|a_{1:t-1})} \right].$$

Taking this further, we employ the same tractable variational distribution drawn from our transition function,

$$I(o_{1:t}; z_{1:t}) \leq \sum_{k=1}^{t-1} \mathbb{E}_{p(z_k, o_k, a_k)} \left[\log \frac{p(z_{k+1}|o_{k+1})}{q_\theta(z_{k+1}|z_k, a_k, h_k)} \right] = I_{\text{LTC}}. \tag{8}$$

This term is an upper-bound for $I(o_{1:t}, z_{1:t})$, quantifying the ratio between the latent representation derived from the encoder and the transitioning state obtained from a past representation when a specific action is applied. Intuitively, this constrains the latent dynamical model (transition function) to diverge minimally from the latent representations obtained from the observation encoder. Hence, we refer to this term as the Latent Consistency Loss $\mathcal{L}_{\text{LTC}}$.

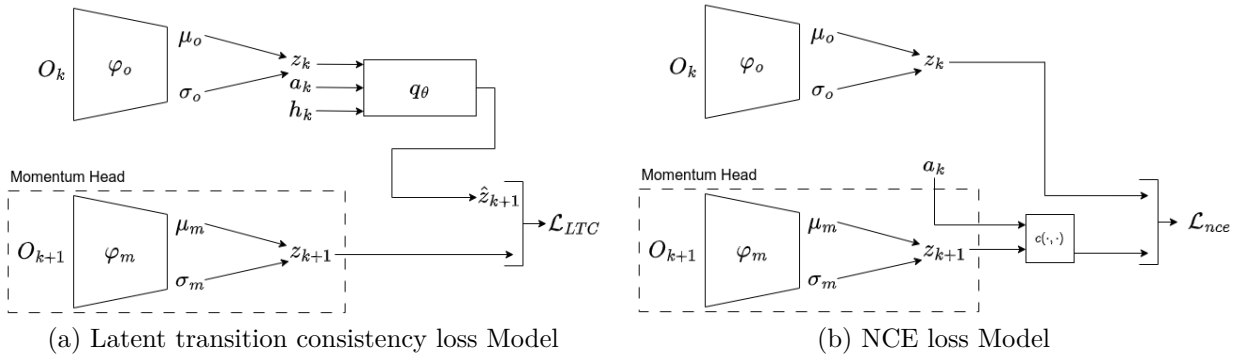(a) Latent transition consistency loss Model   (b) NCE loss Model

Figure 3: Representation of models used for calculating auxiliary losses (a) LTC loss $\mathcal{L}_{LTC}$ and NCE loss ($\mathcal{L}_{NCE}$). Encoder and target encoder parameters are defined as φ_0 and φ_m respectively. a) Once the current representation is obtained, it is passed through the transition function q_θ to obtain the next latent representation, from which the $\mathcal{L}_{LTC}$ is finally calculated (Algorithm 2 in Supplementary material). b) Next latent representation and current action is passed via concatenation function c to obtain unified representation, then compared with current state representation via contrastive learning.

4.3 Maximising the lower bound of the Predictive Mutual Information

This subsection discusses the maximization of the last two terms in the formulation of DePre in Equation 3.

4.3.1 Lower bound of the predictive latent space dynamics.

In order to obtain the lower bound on this MI term, we factorise the transition model by applying the chain rule,

$$
I(z_{t:T}) = \mathbb{E}_{p(z_{t:T})} \left[\log \frac{p(z_{t:T})}{\prod_{k=t}^{T} p(z_k)} \right] = \mathbb{E}_{p(z_{t:T})} \left[\log \prod_{k=t}^{T-1} \frac{p(z_k|z_{k+1:T})}{p(z_k)} \right],
$$

$$
\geq \sum_{k=t}^{T-1} \mathbb{E}_{p(z_k,a_k)} \left[\log \frac{p(z_k|z_{k+1},a_k)}{p(z_k)} \right] = \sum_{k=t}^{T-1} I\big(z_{k+1},a_k;z_k\big). \tag{9}
$$

The mutual information objective $I(z_{k+1},a_k;z_k)$ can be decomposed using the chain rule for mutual information, yielding $I(z_k;z_{k+1}) + I(z_k;a_k|z_{k+1})$. The first component, solely depends on state-transitions. It is closely related to the predictive coding objective (Oord et al., 2018; Anand et al., 2019). Omitting actions could impair the model's capability to determine the optimal actions (Rakelly et al., 2021). The second term can be represented in terms of conditional entropy as $H(a_k|z_k) - H(a_k|z_k,z_{k+1})$. The term $H(a_k|z_k,z_{k+1})$ effectively characterizes the entropy of the inverse dynamics, conceptually aligns closely with an extensive spectrum of prior studies that have focused on exploration and unsupervised learning of representations (Zhang et al., 2018; Pathak et al., 2017; Chandak et al., 2019; Bharadhwaj et al., 2022). Also, this term is the empowerment objective used in InfoPOWER Bharadhwaj et al. (2022). From an intuitive perspective, inverse models operate as an agreement mechanism between the actual and the ground truth action representations. This mechanism enables the representation to capture only those aspects of the state that are essential for predicting the action, thereby discarding potentially irrelevant information. The MI term in Equation 9 can be viewed as a combined objective that optimises state transitions with the regularization of action representations.

For optimising this lower bound, we will utilise contrastive learning (Oord et al., 2018), which yields a variational lower bound of the mutual information in Equation 9. Strategies employed by He et al. (2020); Laskin et al. (2020) relies on data augmentation to generate positive and negative samples. Contrary to them, we take inspiration from Bai et al. (2021) that incorporate policy transitions to obtain these samples. Positive samples are directly acquired by sampling transitions (z_t, a_t, z_{t+1}), while the construction of negative samples involves randomly sampling z_t^* and concatenating it with (a_t, z_{t+1}). As a result, we produce samples (z_t^*, a_t, z_{t+1}) that deviate from the transition dynamics. Thus we obtain MI objective as,

$$
I(z_{k+1},a_k;z_k) \geq \mathbb{E}_{p,N} \left[\log \frac{e^{\sigma(z_k,a_k,z_{k+1})}}{\sum_{z_k^* \in N^- \cup z_k} e^{\sigma(z_k^*,a_k,z_{k+1})}} \right] \triangleq I_{\text{NCE}}, \tag{10}
$$

where N is the set of negative samples and σ is the score function. Score function distinguishes between positive samples (those following the actual transition dynamics) and negative samples (those deviating from these dynamics). It providing high score to the positive examples and low score to the negative examples. It tells how well an action a_k leads to a transition from a latent state z_k to a subsequent latent state z_{k+1}. This evaluation is based on the degree to which the action and the resultant state change are congruent with the expected dynamics of the system. We opt for bilinear products as our score function (Oord et al., 2018; Laskin et al., 2020; Henaff, 2020), which is mathematically defined as $\sigma(z_k,a_k,z_{k+1}) = c(a_t,z_{t+1})^T \mathcal{W} z_t$. The concatenation function $c(\cdot,\cdot)$ is parameterised by a neural network that merges the action a_t with the subsequent latent state z_{t+1} into a single vector (as shown in Figure 3) and $\mathcal{W}$ is the learnable weight matrix.

4.3.2 Lower bound of the predictive observation model.

Directly maximizing $I(z_{t,t^+}; o_{t,t^+})$ is infeasible due to its marginal's intractability. Similar to (Alemi et al., 2017), we propose to optimise a lower bound on our MI,

$$
I(z_{t:T}; o_{t:T}) = \mathbb{E}_{p(z_{t:T}, o_{t:T})} \left[\log \frac{p(o_{t:T}|z_{t:T})}{p(o_{t:T})} \right] = \mathbb{E}_{p(z_{t:T}, o_{t:T})} \left[\log \prod_{k=t}^{T} \frac{p(o_k|z_k)}{p(o_k)} \right],
$$

$$\geq \sum_{k=t}^{T} \mathbb{E}_{p(z_k,o_k)} \left[\log \frac{r_\psi(o_k|z_k)}{p(o_k)} \right],$$

where where $p(o_k|z_k)$ is an intractable conditional distribution and $r_\psi(o_k|z_k)$ is a tractable variational decoder, represented by a neural network with parameters ψ. We rule out the entropy term as it is independent of our optimization procedure,

$$I(z_{t:T}; o_{t:T}) = \sum_{k=t}^{T} \mathbb{E}_{p(z_k,o_k)} \left[\log \ r_\psi(o_k|z_k) \right] = I_{\text{Rec}} . \tag{11}$$

I_{Rec} can be interpreted as the log-likelihood of the observations given the state encodings.

4.4 Combined Objective

Our optimization strategy can be unified into a single objective function as,

$$\min_{\theta,\psi,\phi,\mathcal{W}} \mathcal{L}_{DePre} = [\alpha_1 I_{LTC} + \alpha_2 I_{CLUB}] - [\beta_1 I_{Rec} + \beta_2 I_{NCE}]. \tag{12}$$

The two losses, I_{LTC} and I_{Rec}, are responsible for the representations from the encoder and decoder respectively, while the other two terms, I_{CLUB} and I_{NCE}, formulated as a contrastive loss, control the representations of the transition functions. They are jointly optimized.

4.5 Practical Implementation with Soft-Actor Critic

We jointly train DePre with SAC, an off-policy model-free reinforcement learning method, by incorporating Equation (12) as an auxiliary objective while training the algorithm (Supplementary Material Section 3.1). The transition model, accounting for latent dynamics, is designed to capture the inherent stochasticity of the transitions. It is parameterised with a neural network that returns a Gaussian distribution defined by its mean and variance. The Observation model implemented as a Deconvolutional Neural Network. The History model is implemented as a Gated Recurrent Unit (GRU, Cho et al. (2014)). We utilize a stochastic encoder to obtain representations from the images (Eysenbach et al., 2021; Theis & Agustsson, 2021), parameterised by φ. For encoding subsequent observations, we leverage an exponential moving average of the online network parameters, denoted as φ_m (He et al., 2020). We utilise the same principle for latent targets (Hansen et al., 2022) for transition function, as it should ensure more stable learning process, accommodating any potential fluctuations in the learning (Figure 3). The complete algorithm with SAC is described in the Supplementary material.

5 Experiments

In this section, we conduct a thorough empirical assessment of the proposed DePre method on the DeepMind control suite (DMC, Tassa et al. (2018)) in various settings and compare it with existing state-of-the-art approaches. We evaluate three distinct types of environments: (i) Standard environment with a static background, (ii) Natural environment with video-based, real-world backgrounds, and (iii) Random environment with varying backgrounds in each frame. To underline the significance of each element in the model, we conclude this section with an ablation study.

5.1 Environment Settings

For all three environments, we conducted experiments on six DMC tasks: Cheetah Run, Walker Walk, Cartpole Swingup, Reacher Easy, Pendulum Swingup and Cup Catch. These robot control tasks pose different challenges, such as sparse rewards, contacts and complex dynamics. For the standard settings, no perterbutations are applied to the observations. The observations are RGB images of the size $84 \times 84 \times 3$. By incorporating the ground plane, a substantial portion of the background image is obscured, thereby simplifying the task at hand. Thus, the ground plane is eliminated to maximize the utilization of

the background image. These natural videos are incorporated from Kinetics 400 dataset Kay et al. (2017) at random. We used videos from random categories compared to the simplified challenge in DBC Zhang et al. (2021) who only considered the driving category. Contrary to the predominant use of grayscale images in benchmarking, we employing RGB videos in the background. We independently sampled 100 videos separately for training and testing. More information about the background noise is provided in the Supplementary Material (Section 4.1).

5.2 Baselines and Implementation details

In this evaluation, we compare our approach to a selection of nine most-closely related approaches i.e. Dreamer (Hafner et al., 2020a), Dreamer-V2 (Hafner et al., 2021b), Task-informed Abstractions (TIA, Fu et al. (2021)), Denoised MDPs (Wang et al., 2022), Deep Bisimulation for Control (DBC, Zhang et al. (2021)), Self-Predicting Representations (SPR, Schwarzer et al. (2021)), Variational Sparse Gating (VSG, Jain et al. (2022)), Iso-Dreamer (Pan et al., 2022) and Temporal Predictive Coding (TPC, Nguyen et al. (2021)). These selected methods are distinguished by their superior performance and accompanied by publicly accessible source code. The task return is examined every 1000 steps. For all baseline methods, we employed the optimal set of hyperparameters as indicated in the respective papers. Each task is executed with three different seeds for each model. Detailed explanations of these methods and of the implementations can be found in the Supplementary Material (Section 4).

5.3 Results in Standard Settings

While our main focus isn't on noiseless environments, we evaluated our method against baseline approaches in such settings. We observed that Dreamer outperforms all the methods in most of the environment in these settings. As depicted in Figure 4, our method is competitive in most of the environments.
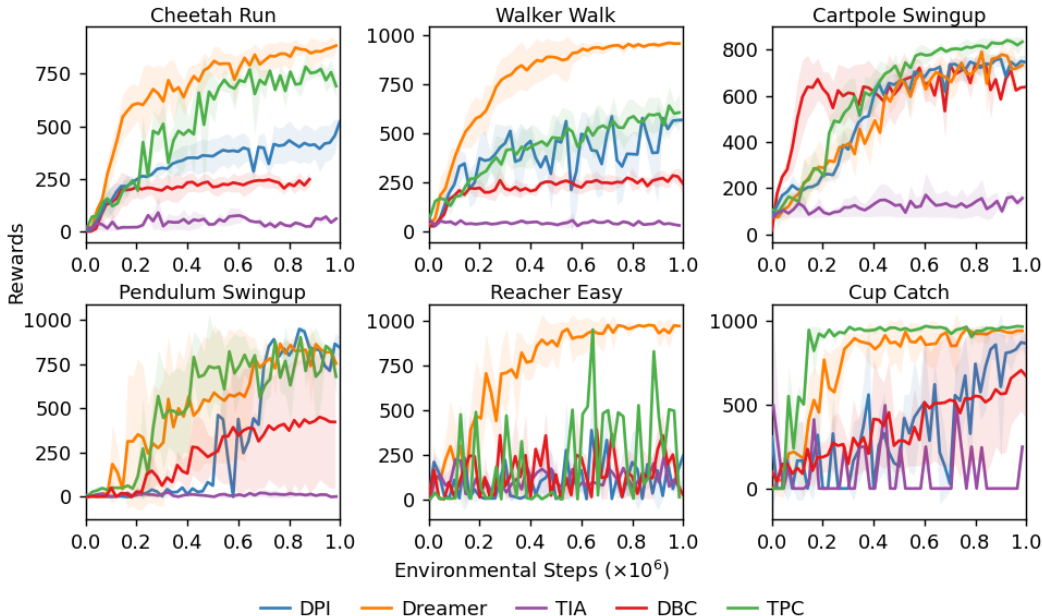

Figure 4: **Standard setting**. Performance comparison of our method (DePre) and baselines on six observation-based continuous control tasks from DMC Suite. Mean of 3 runs; shaded areas are 95% confidence intervals.

5.4 Results in Natural Background settings

Figure 7 illustrates the outcomes when employing natural backgrounds, wherein the background videos were not presented to the agent during its training phase. The main reasons for the degraded performance of most baseline methods was changing the background image to RGB. Dreamer struggles to accurately capture the

agent's entire state, and inadvertently incorporates the irrelevant background noise into its representation (Supplementary Material Section 5). TIA, on the other hand, can only effectively distinguish the agent from the distractor when the background is rendered in grayscale. DBC's performance is on par with these methods, however, it does not achieve the performance that was reported by Zhang et al. (2021). This discrepancy is largely due to the inclusion of RGB image in the background and authors' approach to use the same video for both training and testing, which hampers its capability to manage diverse distraction and restricts its generalization capability to unseen distractions. Similarly, TPC (Nguyen et al., 2021) and Denoised MDPs (Wang et al., 2022) underperformed due to its incapability to generalise to diverse unseen distractions. Our implementation utilises the authors' open-sourced code, with the sole adjustment being the introduction of additional videos. Contrary to these methods, DePre achieves better rewards in the top three environments in Figure 7 (Also see Table 1). These results clearly demonstrate the superior performance of our method, DePre, across the majority of tested environments. This can be attributed to the inclusion of different components in our bottleneck framework which in-turn preserves the predictive information during transitions. Such integration results in a reconstructed scene where the background is blurred, and the agent is enhanced, signifying DePre's capacity to encode task-relevant components, enhancing its performance even in complex and noisy environments (Reconstruction Results in Supp. Material Section 6).

However, it is crucial to note that the results from specific environments - Pendulum Swingup, Reacher Easy, and Cup Catch - do not conclusively reflect the learning effectiveness of any method. During our experiments, we found out the none of the method actually learns the environment and the observed performance is predominantly influenced by the randomness of seed selection. For example, in some scenarios in the Cup Catch environment, episodes often commence with the cup already secured in the holder, leading to an unearned high score of 1000 for the entirety of the episode, unless the agent inadvertently dislodges it. This results in sporadic and misleading evaluation scores, such as $\{1000, 0, 0\}$, averaging to 333 ± 576. Similarly, in the Reacher Easy environment, we observed that VSG, DBC, Iso-Dreamer and DePre, rather than accomplishing the task of reaching, learn to rotate the arm, thereby achieving higher scores compared to other methods that fail even in this unintended task. This observation, however, does not hold true in other environments like Cheetah Run, Walker Walk, and Cartpole Swingup. In the Cartpole Swingup environment, specifically, we noted that if the agent learns merely to rotate the cartpole instead of executing the swingup movement, it attains scores ranging between 150 and 200, a benchmark almost all methods achieved, DePre being the exception, which actually learns to swingup and balance it.

Failure under Sparse rewards. As illustrated in Figure 7, our approach excels in Dense reward scenarios (e.g., Cheetah run, Walker walk, Cartpole swingup). However, it struggles with sparse reward environments (Cup Catch and Pendulum Swingup) after 10^6 environment steps. The complexity of the task, when paired with the visual noise in the environment, presents a considerable challenge and surpasses the limits of current methodologies. In conclusion, the tasks that are inherently hard for model-based methods would remain hard for DePre. Significant improvements can be made for exploration in such environments.

Table 1: Rewards in Natural and Random Environment Background Settings

	Natural Settings						Random Settings	
Method	**Cheetah Run**	**Walker Walk**	**Cartpole Swingup**	**Pendulum Swingup**	**Reacher Easy**	**Cup Catch**	**Cheetah Run**	**Cartpole Swingup**
DBC	122 ± 4	74 ± 41	181 ± 48	$\mathbf{26 \pm 46}$	$\mathbf{305 \pm 470}$	0 ± 0	37 ± 3	268 ± 167
De-MDPs	71 ± 18	113 ± 26	73 ± 2	0 ± 0	83 ± 33	0 ± 0	118 ± 41	149 ± 38
Dreamer	42 ± 9	68 ± 31	109 ± 46	0 ± 0	129 ± 188	68 ± 31	118 ± 41	149 ± 38
Dreamer-V2	118 ± 51	39 ± 29	137 ± 78	0 ± 0	0 ± 0	0 ± 0	155 ± 103	144 ± 38
SPR	45 ± 59	37 ± 6	150 ± 21	7 ± 10	100 ± 78	99 ± 1	105 ± 32	201 ± 18
TIA	20 ± 14	80 ± 52	118 ± 11	0 ± 0	115 ± 161	237 ± 411	16 ± 7	75 ± 2
TPC	42 ± 37	30 ± 9	106 ± 27	25 ± 35	16 ± 3	237 ± 334	59 ± 10	132 ± 97
VSG	56 ± 14	232 ± 43	139 ± 10	0 ± 0	12 ± 17	0 ± 0	127 ± 79	139 ± 10
Iso-Dreamer	10 ± 4	250 ± 48	99 ± 50	0 ± 0	12 ± 3	0 ± 0	5 ± 2	56 ± 27
DePre (Ours)	$\mathbf{263 \pm 11}$	$\mathbf{454 \pm 60}$	$\mathbf{658 \pm 62}$	$\mathbf{40 \pm 57}$	$\mathbf{308 \pm 222}$	$\mathbf{333} \pm \mathbf{576}$	$\mathbf{248 \pm 33}$	$\mathbf{572 \pm 110}$

The table illustrates the rewards obtained in natural and random background settings across a spectrum of tasks. The best or comparable method is present in bold. De-MDPs is shorthand for Denoised MDPs.

5.5 Results in Random Background settings

In this experiment, every time instance features a unique background image, inducing maximum stochasticity in the environment. This experiment illustrates the preservation of temporally predictive information by DePre. As demonstrated in Figure 1, for Cheetah run, DePre effectively isolates task-relevant features, managing to reconstruct only the agent against a randomized background. In Figure 5 and Table 1, a comparative analysis is presented between DePre and nine baseline methodologies in Cheetah Run and Cartpole swingup environment. This shows superior performance of DePre over the baselines in natural background settings. The notable performance drop observed in Denoised MDPs Wang et al. (2022) can be attributed to the introduction of varied and continually changing videos during the evaluation phase. It is likely that it has encountered the frames where the agent is not capable of segregating the relevant components from the non-relevant ones. This issue highlights a key limitation in its robustness and adaptability to varying environments.
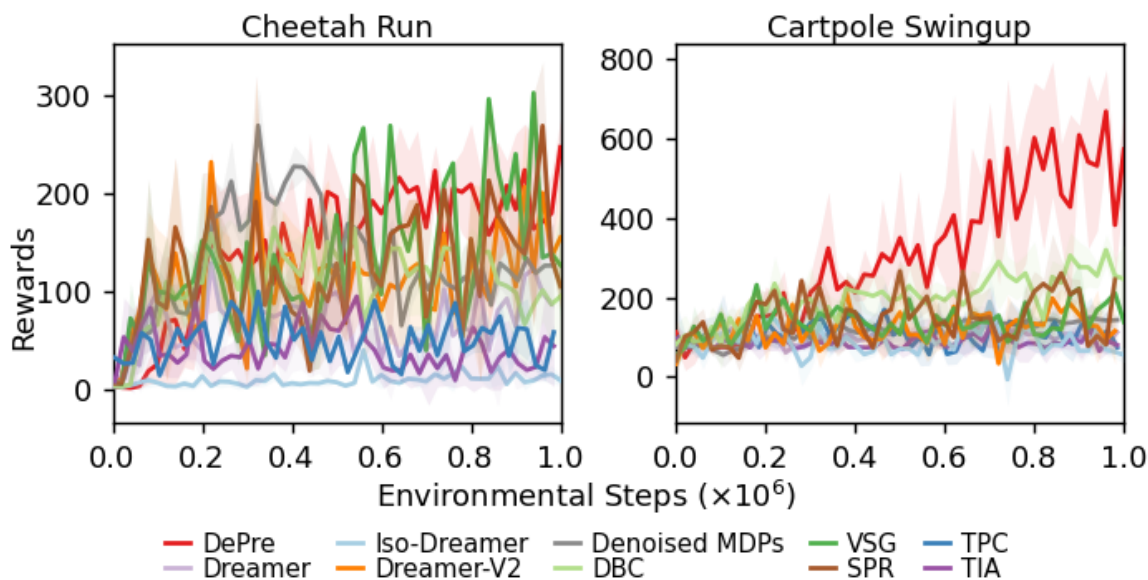

Figure 5: **Random Background Setting**. Comparison of DePre with baselines in random background setting on three runs.
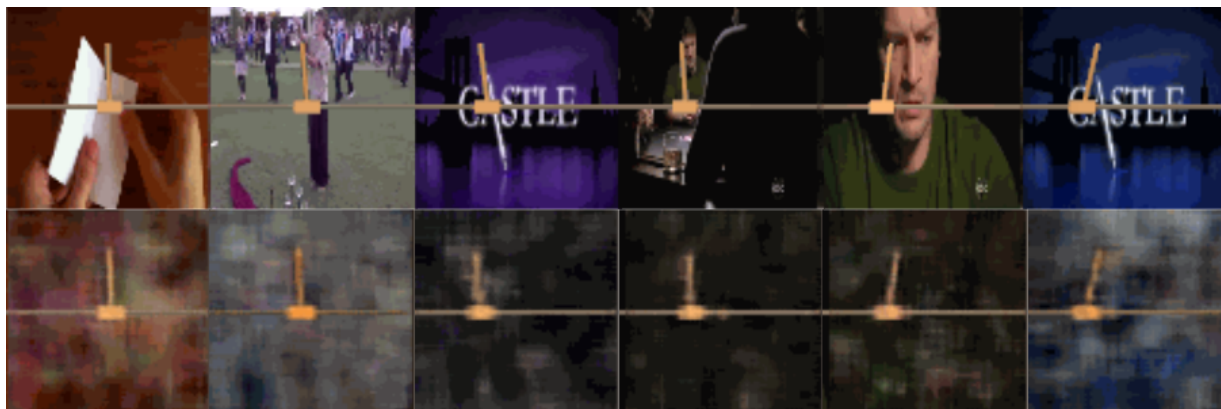

Figure 6: **Reconstruction in cartpole environment in random settings**. Observation reconstruction of DePre in the Cartpole environment in random background setting. First row: Ground Truth, Second row: DePre reconstruction
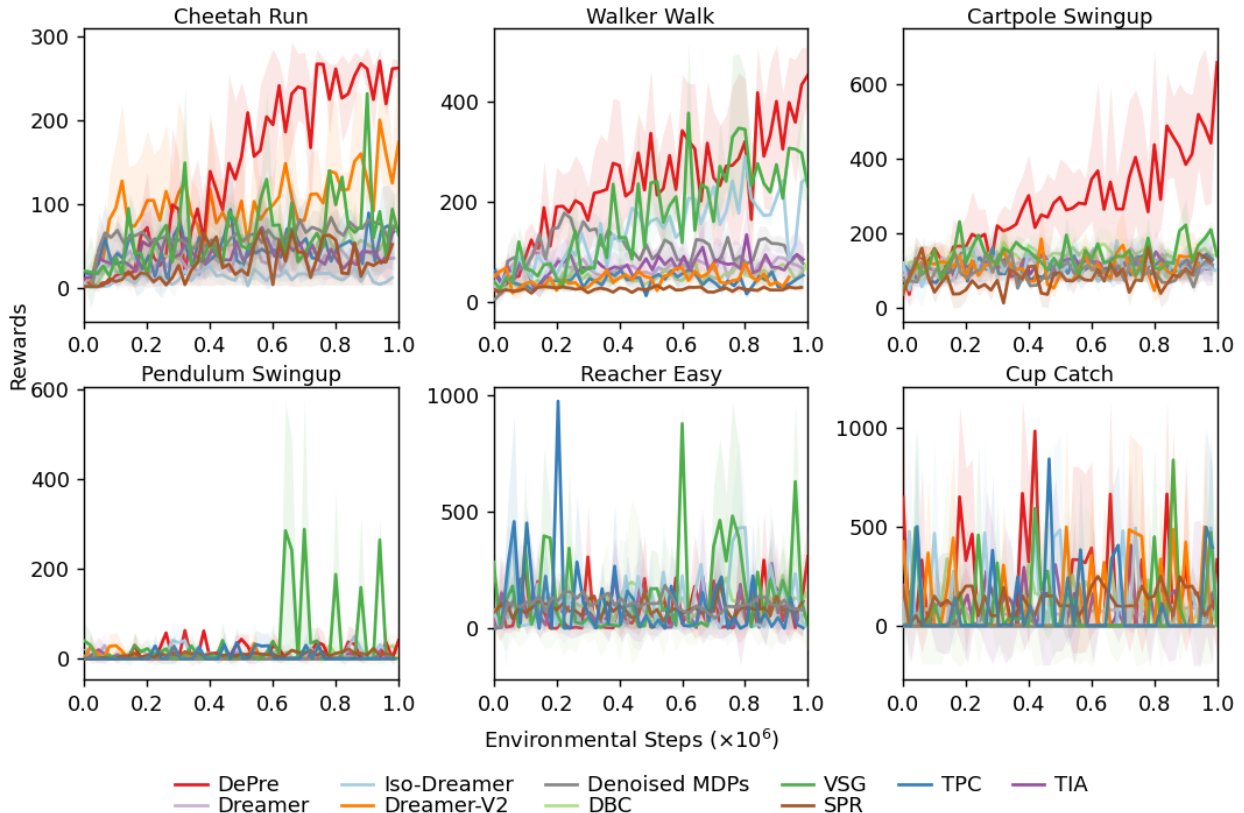
Figure 7: **Natural Background Setting**. Test performance of our method (DePre) and nine baselines on six robot control tasks, with added videos as background noise. Shown is the mean of three runs where shaded areas denote 95% confidence intervals.

6 Discussion and Conclusion

Our work demonstrates that our information-theoretic formulation suggests a pathway to segregate and represent task-relevant information in a noisy world, without explicitly modelling any rules of the MDPs. We also show that objectives related to maximising information on various variables, that are explicitly mentioned in other research (Bai et al., 2021; You et al., 2022; Lee et al., 2020b), implicitly emerge out from our theoretical formulation. In our analysis, all the methodologies exhibit strong performance in noise-free scenarios. When subjected to natural noise scenarios, characterized by real-world videos, DePre consistently either surpassed or equaled the best of nine baselines in performance. However, there's a noticeable path for improvement as every method encountered challenges in tasks dominated by sparse rewards (bottom row of Figure 7). Most notably, in random noise conditions, DePre does not face significant drop in performance and outperforms all other baseline methodologies. We assert that, while there have been notable contributions in the segregation of controllable and non-controllable elements within scenes, the field is in dire need of algorithms that are capable of performing effectively in challenging and complex environments. This necessity is clearly underscored by our empirical analysis, which highlights the current limitations and underscores the importance of continued development in this area.

Our method can be combined with any existing RL model that performs exponentially well in noise-free environment. We believe that there is a great room for improving the performance of our model, e.g., by improving the model architecture for the encoding representations using Resnet like in Bai et al. (2021), by utilising experience replay sampling strategies like PER (Schaul et al., 2016), or by incorporating sophisticated exploration strategies for sparse environments (Laskin et al., 2020; You et al., 2022).

References

Alexander A. Alemi, Ian Fischer, Joshua V. Dillon, and Kevin Murphy. Deep variational information bottleneck. In *International Conference on Learning Representations*, 2017. URL `https://openreview.net/forum?id=HyxQzBceg`.

Ankesh Anand, Evan Racah, Sherjil Ozair, Yoshua Bengio, Marc-Alexandre Côté, and R Devon Hjelm. Unsupervised state representation learning in atari. *Advances in Neural Information Processing Systems (NeurIPS)*, 32, 2019.

Chenjia Bai, Lingxiao Wang, Lei Han, Animesh Garg, Jianye HAO, Peng Liu, and Zhaoran Wang. Dynamic bottleneck for robust self-supervised exploration. In A. Beygelzimer, Y. Dauphin, P. Liang, and J. Wortman Vaughan (eds.), *Advances in Neural Information Processing Systems (NeurIPS)*, 2021. URL `https://openreview.net/forum?id=-t6TeG3A6Do`.

Homanga Bharadhwaj, Mohammad Babaeizadeh, Dumitru Erhan, and Sergey Levine. Information prioritization through empowerment in visual model-based RL. In *International Conference on Learning Representations*, 2022. URL `https://openreview.net/forum?id=DfUjyyRW9O`.

William Bialek and Naftali Tishby. Predictive information. *arXiv preprint cond-mat/9902341*, 1999.

William Bialek, Ilya Nemenman, and Naftali Tishby. Predictability, complexity, and learning. *Neural computation*, 13(11):2409–2463, 2001.

Yash Chandak, Georgios Theocharous, James Kostas, Scott Jordan, and Philip Thomas. Learning action representations for reinforcement learning. In *International Conference on Machine Learning*, pp. 941–950. PMLR, 2019.

Ting Chen, Simon Kornblith, Mohammad Norouzi, and Geoffrey Hinton. A simple framework for contrastive learning of visual representations. In *International Conference on Machine Learning*, pp. 1597–1607. PMLR, 2020.

Kyunghyun Cho, Bart van Merriënboer, Dzmitry Bahdanau, and Yoshua Bengio. On the properties of neural machine translation: Encoder–decoder approaches. In *Proceedings of SSST-8, Eighth Workshop on Syntax, Semantics and Structure in Statistical Translation*, pp. 103–111, Doha, Qatar, October 2014. Association for Computational Linguistics. doi: 10.3115/v1/W14-4012. URL `https://aclanthology.org/W14-4012`.

Kurtland Chua, Roberto Calandra, Rowan McAllister, and Sergey Levine. Deep reinforcement learning in a handful of trials using probabilistic dynamics models. *Advances in Neural Information Processing Systems (NeurIPS)*, 31, 2018.

Yiming Ding, Ignasi Clavera, and Pieter Abbeel. Mutual information maximization for robust plannable representations. *arXiv preprint arXiv:2005.08114*, 2020.

Frederik Ebert, Chelsea Finn, Sudeep Dasari, Annie Xie, Alex Lee, and Sergey Levine. Visual foresight: Model-based deep reinforcement learning for vision-based robotic control. *arXiv preprint arXiv:1812.00568*, 2018.

Ben Eysenbach, Russ R Salakhutdinov, and Sergey Levine. Robust predictable control. *Advances in Neural Information Processing Systems (NeurIPS)*, 34:27813–27825, 2021.

Xiang Fu, Ge Yang, Pulkit Agrawal, and Tommi Jaakkola. Learning task informed abstractions. In Marina Meila and Tong Zhang (eds.), *Proceedings of the 38th International Conference on Machine Learning*, volume 139 of *Proceedings of Machine Learning Research*, pp. 3480–3491. PMLR, 18–24 Jul 2021. URL `http://proceedings.mlr.press/v139/fu21b.html`.

Carles Gelada, Saurabh Kumar, Jacob Buckman, Ofir Nachum, and Marc G Bellemare. Deepmdp: Learning continuous latent space models for representation learning. In *International Conference on Machine Learning*, pp. 2170–2179. PMLR, 2019.

David Ha and Jürgen Schmidhuber. Recurrent world models facilitate policy evolution. In S. Bengio, H. Wallach, H. Larochelle, K. Grauman, N. Cesa-Bianchi, and R. Garnett (eds.), *Advances in Neural Information Processing Systems (NeurIPS)*, volume 31. Curran Associates, Inc., 2018. URL `https://proceedings.neurips.cc/paper_files/paper/2018/file/2de5d16682c3c35007e4e92982f1a2ba-Paper.pdf`.

Danijar Hafner, Timothy Lillicrap, Ian Fischer, Ruben Villegas, David Ha, Honglak Lee, and James Davidson. Learning latent dynamics for planning from pixels. In *International Conference on Machine Learning*, pp. 2555–2565. PMLR, 2019.

Danijar Hafner, Timothy Lillicrap, Jimmy Ba, and Mohammad Norouzi. Dream to control: Learning behaviors by latent imagination. In *International Conference on Learning Representations*, 2020a. URL `https://openreview.net/forum?id=S1lOTC4tDS`.

Danijar Hafner, Pedro A Ortega, Jimmy Ba, Thomas Parr, Karl Friston, and Nicolas Heess. Action and perception as divergence minimization. *arXiv preprint arXiv:2009.01791*, 2020b.

Danijar Hafner, Timothy P Lillicrap, Mohammad Norouzi, and Jimmy Ba. Mastering atari with discrete world models. In *International Conference on Learning Representations*, 2021a. URL `https://openreview.net/forum?id=0oabwyZbOu`.

Danijar Hafner, Timothy P Lillicrap, Mohammad Norouzi, and Jimmy Ba. Mastering atari with discrete world models. In *International Conference on Learning Representations*, 2021b. URL `https://openreview.net/forum?id=0oabwyZbOu`.

Nicklas Hansen, Xiaolong Wang, and Hao Su. Temporal difference learning for model predictive control. In *International Conference on Machine Learning*. PMLR, 2022.

Kaiming He, Haoqi Fan, Yuxin Wu, Saining Xie, and Ross Girshick. Momentum contrast for unsupervised visual representation learning. In *Proceedings of the IEEE/CVF conference on computer vision and pattern recognition*, pp. 9729–9738, 2020.

Olivier Henaff. Data-efficient image recognition with contrastive predictive coding. In *International Conference on Machine Learning*, pp. 4182–4192. PMLR, 2020.

R Devon Hjelm, Alex Fedorov, Samuel Lavoie-Marchildon, Karan Grewal, Phil Bachman, Adam Trischler, and Yoshua Bengio. Learning deep representations by mutual information estimation and maximization. In *International Conference on Learning Representations*, 2019. URL `https://openreview.net/forum?id=Bklr3j0cKX`.

Riashat Islam, Manan Tomar, Alex Lamb, Hongyu Zang, Yonathan Efroni, Dipendra Misra, Aniket Rajiv Didolkar, Xin Li, Harm van Seijen, Remi Tachet des Combes, and John Langford. Agent-controller representations: Principled offline RL with rich exogenous information. In *3rd Offline RL Workshop: Offline RL as a "Launchpad"*, 2022. URL `https://openreview.net/forum?id=0pFzg-8y-o`.

Arnav Kumar Jain, Shivakanth Sujit, Shruti Joshi, Vincent Michalski, Danijar Hafner, and Samira Ebrahimi Kahou. Learning robust dynamics through variational sparse gating. In *Advances in Neural Information Processing Systems*, December 2022.

Lukasz Kaiser, Mohammad Babaeizadeh, Piotr Miłos, Błażej Osiński, Roy H Campbell, Konrad Czechowski, Dumitru Erhan, Chelsea Finn, Piotr Kozakowski, Sergey Levine, Afroz Mohiuddin, Ryan Sepassi, George Tucker, and Henryk Michalewski. Model based reinforcement learning for atari. In *International Conference on Learning Representations*, 2020. URL `https://openreview.net/forum?id=S1xCPJHtDB`.

Will Kay, Joao Carreira, Karen Simonyan, Brian Zhang, Chloe Hillier, Sudheendra Vijayanarasimhan, Fabio Viola, Tim Green, Trevor Back, Paul Natsev, et al. The kinetics human action video dataset. *arXiv preprint arXiv:1705.06950*, 2017.

Michael Laskin, Aravind Srinivas, and Pieter Abbeel. Curl: Contrastive unsupervised representations for reinforcement learning. In *International Conference on Machine Learning*, pp. 5639–5650. PMLR, 2020.

Alex X. Lee, Anusha Nagabandi, Pieter Abbeel, and Sergey Levine. Stochastic latent actor-critic: Deep reinforcement learning with a latent variable model. In *Advances in Neural Information Processing Systems (NeurIPS)*, 2020a.

Kuang-Huei Lee, Ian Fischer, Anthony Liu, Yijie Guo, Honglak Lee, John Canny, and Sergio Guadarrama. Predictive information accelerates learning in rl. *Advances in Neural Information Processing Systems (NeurIPS)*, 33:11890–11901, 2020b.

Timothy P. Lillicrap, Jonathan J. Hunt, Alexander Pritzel, Nicolas Heess, Tom Erez, Yuval Tassa, David Silver, and Daan Wierstra. Continuous control with deep reinforcement learning. In Yoshua Bengio and Yann LeCun (eds.), *4th International Conference on Learning Representations, ICLR 2016, San Juan, Puerto Rico, May 2-4, 2016, Conference Track Proceedings*, 2016. URL `http://arxiv.org/abs/1509.02971`.

Yuren Liu, Biwei Huang, Zhengmao Zhu, Honglong Tian, Mingming Gong, Yang Yu, and Kun Zhang. Learning world models with identifiable factorization. *Advances in Neural Information Processing Systems*, 36, 2024.

Kendall Lowrey, Aravind Rajeswaran, Sham Kakade, Emanuel Todorov, and Igor Mordatch. Plan online, learn offline: Efficient learning and exploration via model-based control. In *International Conference on Learning Representations*, 2019. URL `https://openreview.net/forum?id=Byey7n05FQ`.

Xiao Ma, Siwei Chen, David Hsu, and Wee Sun Lee. Contrastive variational reinforcement learning for complex observations. In *Conference on Robot Learning*, pp. 959–972. PMLR, 2021.

Tung D Nguyen, Rui Shu, Tuan Pham, Hung Bui, and Stefano Ermon. Temporal predictive coding for model-based planning in latent space. In *International Conference on Machine Learning*, pp. 8130–8139. PMLR, 2021.

Aaron van den Oord, Yazhe Li, and Oriol Vinyals. Representation learning with contrastive predictive coding. *arXiv preprint arXiv:1807.03748*, 2018.

Minting Pan, Xiangming Zhu, Yunbo Wang, and Xiaokang Yang. Iso-dream: Isolating and leveraging noncontrollable visual dynamics in world models. In *Advances in Neural Information Processing Systems*, 2022.

Deepak Pathak, Pulkit Agrawal, Alexei A. Efros, and Trevor Darrell. Curiosity-driven exploration by self-supervised prediction. In Doina Precup and Yee Whye Teh (eds.), *Proceedings of the 34th International Conference on Machine Learning*, volume 70 of *Proceedings of Machine Learning Research*, pp. 2778–2787. PMLR, 06–11 Aug 2017. URL `https://proceedings.mlr.press/v70/pathak17a.html`.

Kate Rakelly, Abhishek Gupta, Carlos Florensa, and Sergey Levine. Which mutual-information representation learning objectives are sufficient for control?, 2021.

Tom Schaul, John Quan, Ioannis Antonoglou, and David Silver. Prioritized experience replay, 2016.

Max Schwarzer, Ankesh Anand, Rishab Goel, R Devon Hjelm, Aaron Courville, and Philip Bachman. Data-efficient reinforcement learning with self-predictive representations. In *International Conference on Learning Representations*, 2021. URL `https://openreview.net/forum?id=uCQfPZwRaUu`.

Rui Shu, Tung Nguyen, Yinlam Chow, Tuan Pham, Khoat Than, Mohammad Ghavamzadeh, Stefano Ermon, and Hung Bui. Predictive coding for locally-linear control. In *International Conference on Machine Learning*, pp. 8862–8871. PMLR, 2020.

Yuval Tassa, Yotam Doron, Alistair Muldal, Tom Erez, Yazhe Li, Diego de Las Casas, David Budden, Abbas Abdolmaleki, Josh Merel, Andrew Lefrancq, et al. Deepmind control suite. *arXiv preprint arXiv:1801.00690*, 2018.

L. Theis and E. Agustsson. On the advantages of stochastic encoders. In *Neural Compression Workshop at International Conference on Learning Representations*, 2021. URL `https://arxiv.org/abs/2102.09270`.

Yonglong Tian, Dilip Krishnan, and Phillip Isola. Contrastive multiview coding. In *Computer Vision–ECCV 2020: 16th European Conference, Glasgow, UK, August 23–28, 2020, Proceedings, Part XI 16*, pp. 776–794. Springer, 2020.

Naftali Tishby, Fernando C Pereira, and William Bialek. The information bottleneck method. *arXiv preprint physics/0004057*, 2000.

Manan Tomar, Riashat Islam, Sergey Levine, and Philip Bachman. Ignorance is bliss: Robust control via information gating. *arXiv preprint arXiv:2303.06121*, 2023.

Tongzhou Wang, Simon S. Du, Antonio Torralba, Phillip Isola, Amy Zhang, and Yuandong Tian. Denoised mdps: Learning world models better than the world itself. In *International Conference on Machine Learning*. PMLR, 2022.

Denis Yarats, Amy Zhang, Ilya Kostrikov, Brandon Amos, Joelle Pineau, and Rob Fergus. Improving sample efficiency in model-free reinforcement learning from images. In *Proceedings of the AAAI Conference on Artificial Intelligence*, volume 35, pp. 10674–10681, 2021.

Bang You, Jingming Xie, Youping Chen, Jan Peters, and Oleg Arenz. Self-supervised sequential information bottleneck for robust exploration in deep reinforcement learning. *arXiv preprint arXiv:2209.05333*, 2022.

Amy Zhang, Harsh Satija, and Joelle Pineau. Decoupling dynamics and reward for transfer learning, 2018. URL https://openreview.net/forum?id=H1aoddyvM.

Amy Zhang, Rowan Thomas McAllister, Roberto Calandra, Yarin Gal, and Sergey Levine. Learning invariant representations for reinforcement learning without reconstruction. In *International Conference on Learning Representations*, 2021. URL https://openreview.net/forum?id=-2FCwDKRREu.

Marvin Zhang, Sharad Vikram, Laura Smith, Pieter Abbeel, Matthew Johnson, and Sergey Levine. SOLAR: Deep structured representations for model-based reinforcement learning. In Kamalika Chaudhuri and Ruslan Salakhutdinov (eds.), *Proceedings of the 36th International Conference on Machine Learning*, volume 97 of *Proceedings of Machine Learning Research*, pp. 7444–7453. PMLR, 09–15 Jun 2019. URL https://proceedings.mlr.press/v97/zhang19m.html.